

THE INFLUENCE OF COMPOSITION AND GRAIN SIZE ON THE MARTENSITIC TRANSFORMATION  
TEMPERATURES OF Cu-Al-Mn SHAPE MEMORY ALLOYS

C. López del Castillo\*, B.G. Mellor+, M.L. Blázquez\*, and C. Gómez\*

\* Departamento de Ciencias de los Materiales e Ingeniería Metalúrgica,  
Universidad Complutense, 28040 Madrid, Spain.

+Engineering Materials, The University of Southampton, Southampton, SO9 5NH, U.K.

(Received September 7, 1987)

Introduction

Shape memory effect, SME, alloys have been studied for the last twenty-five years and SME devices made from Ni-Ti (Nitinol) and copper-based ternary alloys are commercially available. Copper-based systems are considerably cheaper and easier to fabricate than Nitinol although the shape memory properties of the two ternary systems most studied, Cu-Zn-Al and Cu-Al-Ni, are somewhat inferior to those of Nitinol (1-3). In addition a successful shape memory alloy must be able to be cycled repeatedly through the transformation temperatures without showing any microstructural degradation which would impair shape memory, i.e. ageing phenomena should not take place during service.

Manganese lowers the eutectoid decomposition temperature in copper-based alloys (5-7) which suggests that the  $\beta$  phase in Cu-Al-Mn alloys might be more stable to diffusional decomposition than other copper based alloys. Thus, there has recently been interest in Cu-Al-Mn alloys, the  $\beta$  phase of which, like Cu-Zn-Al and Cu-Al-Ni alloys, undergoes a thermoelastic martensite reaction (8). These alloys have been shown to possess an appreciable SME (9-13).

A knowledge of the dependence of martensitic transformation temperatures on composition is obviously fundamental if practical SME devices are to be made from Cu-Al-Mn alloys. Hence, the present study gives the results of a systematic investigation of the influence of both aluminium and manganese on the martensitic transformation start temperature,  $M_s$ , of Cu-Al-Mn alloys of composition indicated on the section of the Cu-Al-Mn ternary diagram given in Figure 1. This, together with data previously published (6,7,14), then allows the  $M_s$  temperature of Cu-Al-Mn alloys of between 10-14 wt% Al and 0-9 wt% Mn to be estimated.

Grain size has been shown to affect the martensitic transformation temperatures in Cu-Zn-Al and Cu-Al-Ni alloys (15,16). Hence, the grain growth kinetics and the effect of grain size on  $M_s$  temperatures has also been studied in the range of grain sizes available from the chill cast material.

Experiment and Results

Alloys were obtained by induction melting the constituent pure elements in a high frequency furnace followed by chill casting. Their composition was accurately determined by atomic absorption spectroscopy. After casting, sections from the alloys were metallographically prepared by electropolishing using a phosphoric acid, water and ethanol mixture (1:2:1) followed by etching with acidified ferric chloride. As the aluminium and manganese content increased, the martensite plates tended to become thicker with a higher density of internal twinning as can be appreciated from Figures 2-5.

For samples which were  $\beta$  phase at room temperature, e.g. a Cu-12.2 wt% Al-7.6 wt% Mn alloy, optical metallography revealed an average grain size, determined by the linear intercept method, of approximately 120 $\mu$ m. The evolution of the grain size during homogenisation at 800°C was studied in this alloy by holding specimens for various times at that temperature followed by quenching and subsequent metallography. Figure 6 shows the evolution of grain size with homogenisation time,  $t$ ,  $\log D/D_0$  being plotted against  $\log t$  where  $D$  is the average grain size

of the sample after  $t$  minutes at  $800^{\circ}\text{C}$  and  $D_0$  is the original grain size. As can be seen, rapid grain growth occurs during the first 7 minutes at  $800^{\circ}\text{C}$  after which the grain size only slowly increases with time. Superimposed upon this diagram are typical grain structures after various times at  $800^{\circ}\text{C}$ .

The characteristic temperatures of the martensitic and reverse transformations were determined by means of measuring the variation of resistivity with temperature (9,12,18). Electrical connections between the sample and measurement leads were spot-welded so as to eliminate contact resistances which had been previously shown to give rise to spurious results (9). The specimens so prepared were maintained at  $800^{\circ}\text{C}$  in the  $\beta$  phase region (5) for ten minutes followed by water quenching at  $20^{\circ}\text{C}$ . The specimens were held at  $25^{\circ}\text{C}$  for three days followed by thermal cycling between  $-50$  and  $300^{\circ}\text{C}$ . The values taken to characterise the transformation temperatures were those registered in the fourth thermal cycle when any stabilisation effects found in these alloys after quenching in high vacancy concentrations and/or ageing at room temperature prior to the test had been eliminated by the thermal cycling treatment (9,12).

The effect of grain size on the martensitic and reverse transformation temperatures was determined by measuring these temperatures as a function of annealing time at  $800^{\circ}\text{C}$  (i.e. as a function of grain size) for an alloy of composition Cu-10.7 wt%Al -7.5 wt%Mn. No appreciable variations of these temperatures were observed and so it can be concluded that for a grain size of greater than  $120\ \mu\text{m}$  the transformation temperatures are independent of grain size. Similar results were found for Cu-Zn-Al, Cu-Al-Ni and Fe-Ni-C alloys, when the grain size was above  $100\ \mu\text{m}$  (15,16).

In order to study the influence of aluminium and manganese contents on the transformation temperatures, two series of alloys were chosen, as shown in Figure 1. In one series the aluminium was held constant at both 10.6 and 10.7 wt% while the manganese content was varied. In the other series the manganese content was held constant and the aluminium content varied. Table 1 gives the compositions studied and the  $M_s$  temperatures experimentally obtained.

TABLE 1  
Composition of the alloys studied and their  $M_s$  Temperatures

Series	Alloy	Composition wt%			$M_s$ $^{\circ}\text{C}$
		Copper	Aluminium	Manganese	
1	A 20	84.2	10.7	5.1	122
	A 19	84.0	10.7	5.3	112
	A 16	83.5	10.6	5.9	107
	A 21	83.3	10.6	6.1	98
	A 18	82.5	10.6	6.9	54
	A 22	82.4	10.6	7.0	52
	A 17	81.8	10.7	7.5	17
2	A 8	82.6	10.4	7.0	81
	A 22	82.4	10.6	7.0	52
	A 9	82.3	10.7	7.0	45
	A 13	82.1	11.0	6.9	5
	A 7	81.9	11.1	7.0	-10

These temperatures were measured to an accuracy of  $2^{\circ}\text{C}$ . Figures 7 and 8 show the  $M_s$  temperature as a function of the manganese and aluminium contents, respectively, for the two series of alloys. Over these narrow composition ranges the  $M_s$  temperature is seen to decrease

linearly with an increase in aluminium or manganese content when the other element is held constant. Aluminium has a greater effect than manganese, an increase of 1 wt% Al giving rise to a decrease in  $M_S$  temperature of 126°C. The effect of adding 1 wt% Mn is seen to depend somewhat on the aluminium content. Thus, regression analysis revealed that at 10.6 wt Al, 1 wt% Mn increase decreases the  $M_S$  by 51°C, whilst at 10.7 wt% Al, 1 wt% Mn increase decreases the  $M_S$  by 42°C.

A linear regression analysis was conducted to correlate all the  $M_S$  temperatures found in this study to the composition and the following empirical relationship derived:

$$M_S = 1710 - 127.4\% \text{ Al} - 43.6\% \text{ Mn},$$

the aluminium and manganese contents being in wt%. This equation generates the  $M_S$  temperature of all the alloys studied to within  $\pm 5^\circ\text{C}$ .

Figure 9, of  $M_S$  temperature as a function of chemical composition, gives the present results together with those of previous workers. It should be noted that most of the previous studies have determined the  $M_S$  temperature either after quenching from the  $\beta$  field or after holding at room temperature for varying times. Hence, the values of these  $M_S$  temperatures may well have been influenced somewhat by excess vacancy concentrations and stabilisation effects. However from such combined data as those given in Figure 9, the  $M_S$  temperature of a Cu-Al-Mn alloy with an aluminium content of between 10 and 14 wt% and manganese content of 0-9% can be estimated. Over such a wide compositional range, the simple empirical relationship derived from the present data would not be expected to hold with any accuracy. Nevertheless, this empirical linear relationship may be used in alloy development to predict  $M_S$  temperatures quite accurately over albeit a relatively restricted compositional range, but over an  $M_S$  temperature range of  $\sim 100^\circ\text{C}$ .

#### Conclusions

The  $M_S$  temperatures of the Cu-Al-Mn alloys studied do not vary with grain size at least when the average grain size is greater than 120 $\mu\text{m}$ .

$M_S$  temperature determinations carried out on two series of alloys where the aluminium or manganese contents have remained constant indicate that an increase in 1 wt% Mn gives rise to a decrease in the  $M_S$  temperature of 42-51°C, while the same increase in the aluminium content gives rise to a decrease in  $M_S$  of 126°C. A simple linear relationship was found to hold between the  $M_S$  temperatures and composition over a relatively narrow composition range.

#### References

1. L. Delaey, R. Krishnan, H. Tas and M. Warlimont, *J. Mater. Sci.*, 9, 1521-1555, (1974).
2. J. Perkins (ed.), *Shape Memory Effects in Alloys*, New York, Plenum Press, (1975).
3. R.A. Jago (ed.), *Shape Memory Alloys*, *Met. Forum*, 4, (1981).
4. L. Delaey, J. Van Humbeeck, M. Chandrasekaran, J. Janssen, M. Andrade and M. Mwamba, *Met. Forum*, 4, 164-175, (1981).
5. D.R.F. West and D. Lloyd Thomas, *J. Inst. Metals*, 85, (3), 97-112, (1956-67).
6. S.J.L. Kang, M. Stasi and P. Azou, *Mem. Etud. Sci. Rev. Metall.*, 79,(5), 229-234, (1982).
7. I.A. Arbuzova, P.V. Titov and L.G. Khandros, *Akad. Nauk. Ukr. SSR, Metallofiz*, 69, 86-87, (1977).
8. V.A. Lobodyuk, V.V. Martynov, V.R. Tzachuk and L.G. Khandros, *Akad. Nauk. Ukr., SSR, Metallofiz*, 63, 55-60, (1976).
9. C. Lopez del Castillo, *Doctoral Thesis*, Universidad Complutense, Madrid, Spain, (1984).
10. B.G. Mellor, C. Lopez del Castillo and J. Hernaez, *V Assembly of CENIM*, Madrid, Spain, (1981).
11. C. Lopez del Castillo, B.G. Mellor and J. Hernaez, *VI Assembly of CENIM*, Madrid, Spain, (1985).
12. C. Lopez del Castillo, J. Hernaez and B.G. Mellor, *J. Mater. Sci.*, 21, 4043-4047, (1986).

13. B.G. Mellor, J. Hernaez and C. Lopez del Castillo, *Scripta Metall.*, 20, 839-841, (1986).
14. K. Matsushita, T. Okamoto and T. Okamoto, *J. Mater. Sci.*, 20, 689-699, (1985).
15. Dewa N. Adnyana, *Metallography*, 19(2), 187-196, (1986).
16. C. Hayzelden and B. Cantor, *Acta Metall.*, 34(2), 233-242, (1986).
17. J. Hernaez, C. Lopez del Castillo, B.G. Mellor, A.J. Criado and M.L. Blazquez, *Rev. Metall., Madrid*, 22(5), 292-295, (1986).

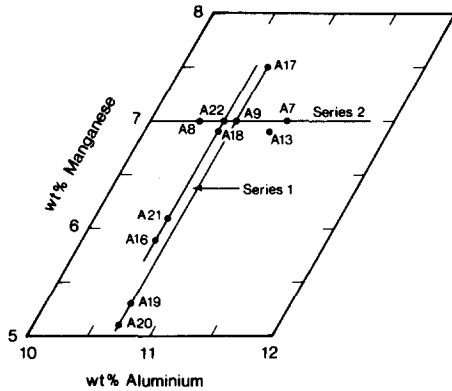


FIG. 1 Position of the alloys studied in the ternary phase diagram.

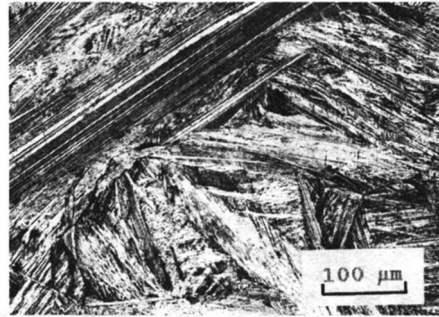


FIG. 2 Microstructure of the Cu-10.7%Al - 5.1%Mn alloy. Note the fine martensitic plates.

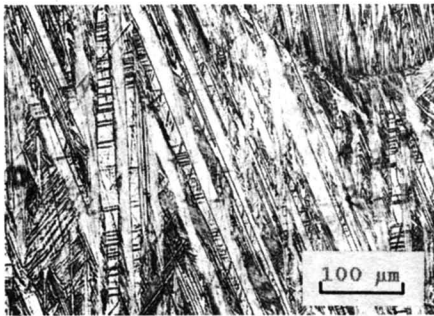


FIG. 3 Microstructure of the Cu-10.6%Al - 7%Mn alloy. Note the thicker, more heavily twinned martensitic plates in this alloy which has a higher manganese content than that of Fig. 2.

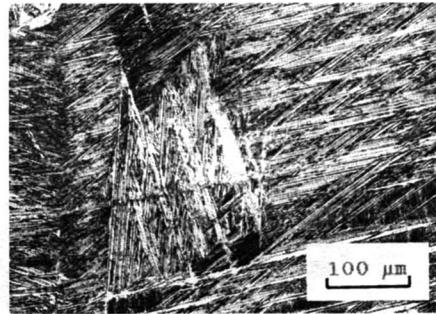


FIG. 4 Microstructure of the Cu-10.4%Al - 7%Mn alloy. Note the fine martensitic plates.

FIG. 5 Microstructure of the Cu-11%Al - 6.9%Mn alloy. Note the thick heavily twinned martensitic plates in this partially martensitic at room temperature alloy, which has a higher aluminium content than that of Fig. 4.



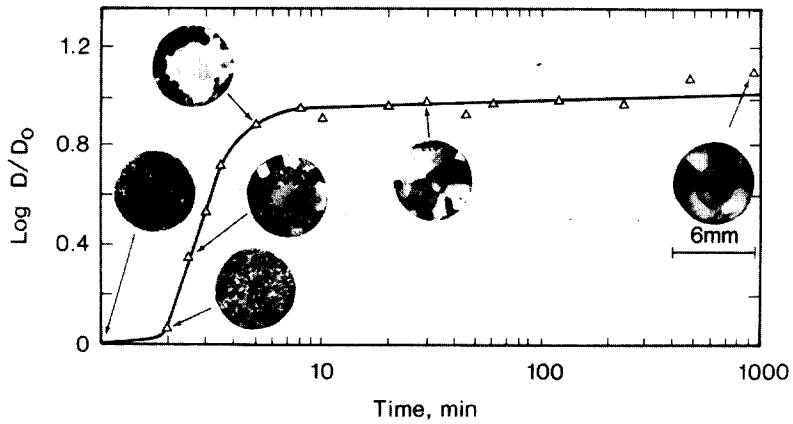


FIG. 6 Evolution of the grain size,  $D$ , as a function of time,  $t$ , at  $800^\circ\text{C}$  for an alloy of composition  $\text{Cu-12.2\%Al - 7.6\%Mn}$ .  $D_0$  is the original grain size.

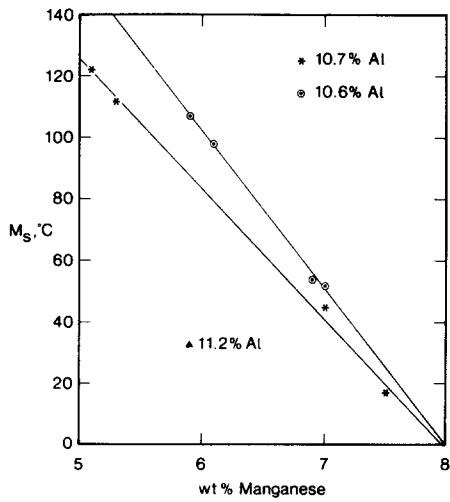


FIG. 7 Variation of  $M_s$  temperature as a function of the manganese content.

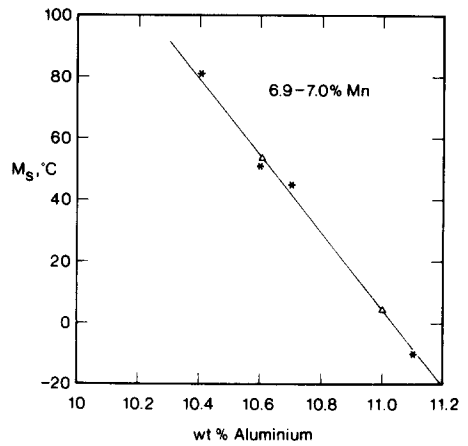


FIG. 8 Variation of  $M_s$  temperature as a function of the aluminium content.

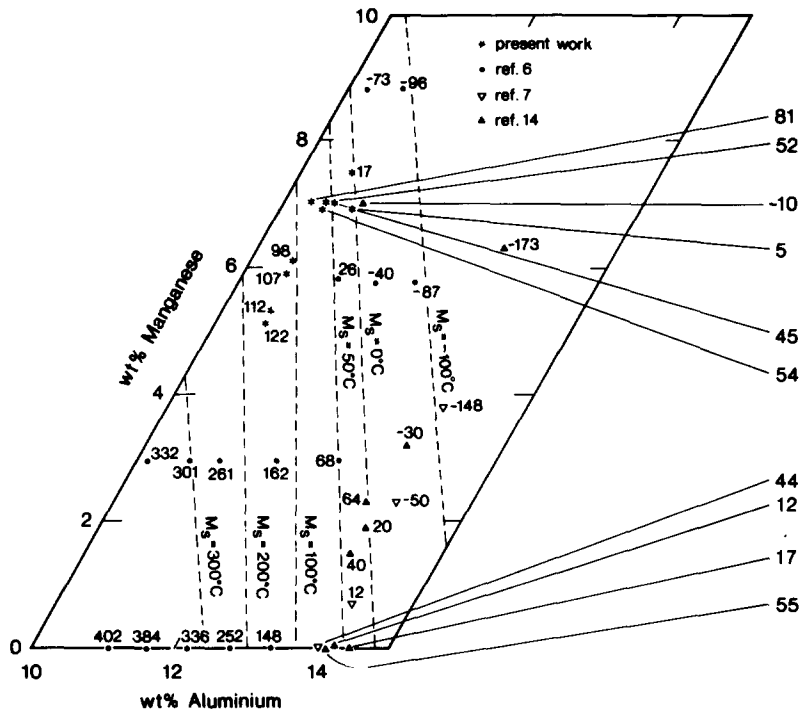


FIG. 9 Estimated  $M_s$  temperature contour lines based on the present and previously published data. Numbers refer to  $M_s$  temperatures in  $^{\circ}\text{C}$ .